Coherency and connectivity in oscillating neural networks: linear partialization analysis

Kalitzin, A.; van Dijk, B.W.; Spekreijse, H.; van Leeuwen, W.A.

DOI
10.1007/s004220050322

Publication date
1997

Document Version
Final published version

Published in
Biological Cybernetics

Biol. Cybern. 76, 73–82 (1997)

Biological Cybernetics

Coherency and connectivity in oscillating neural networks: linear partialization analysis

S. Kalitzin[1,2], Bob W. van Dijk[1,2], H. Spekreijse[1,2], W. A. van Leeuwen[3]

[1] Graduate School of Neurosciences Amsterdam, The Netherlands Ophthalmic Research Institute, Department of Visual Systems Analysis, P.O. Box 12141, 1100 AC Amsterdam, The Netherlands
[2] Laboratory for Medical Physics, UvA, Meibergdreef 9, 1105 AZ Amsterdam, The Netherlands
[3] Institute for Theoretical Physics, University of Amsterdam, Valckenierstraat 65, 1018 XE Amsterdam, The Netherlands

Received: 20 October 1995 / Accepted in revised form: 20 May 1996

Abstract. This paper studies the relation between the functional synaptic connections between two artificial neural networks and the correlation of their spiking activities. The model neurons had realistic non-oscillatory dynamic properties and the networks showed oscillatory behavior as a result of their internal synaptic connectivity. We found that both excitation and inhibition cause phase locking of the oscillating activities. When the two networks excite each other the oscillations synchronize with zero phase lag, whereas mutual inhibition between the networks resulted in an anti-phase (half period phase difference) synchronization. Correlations between the activities of the two networks can also be caused by correlated external inputs driving the systems (common input). Our analysis shows that when the networks exhibit oscillatory behavior and the rate of the common input is smaller than a characteristic network oscillator frequency, the cross-correlation functions between the activities of two systems still carry information about the mutual synaptic connectivity. This information can be retrieved with linear partialization, removing the influence of the common input. We further explored the network responses to periodic external input. We found that when the input is of a frequency smaller than a certain threshold, the network responds with bursts at the same frequency as the input. Above the threshold, the network responds with a fraction of the input frequency. This frequency threshold, characterizing the oscillatory properties of the network, is also found to determine the limit to which linear partialization works.

1 Introduction

Phenomena of correlated neural electrical activity have been extensively studied in experiments measuring single unit activity, multiple unit activity or electroencephalographic signals (Eckhorn et al. 1992; Gray et al. 1992; Nelson et al. 1992; Spekreijse et al. 1994). For a recent review see Singer (1993). In many of these studies authors assume or imply that correlated neural activity expresses the functional connectivity between the corresponding neurons or groups of neurons.

The relation between correlated neural activity and functional connectivity has been rigorously tested in cases of coupled stochastic systems (Aertsen and Gerstein 1985). In this paper we explore this link by simulating biologically realistic signals from artificial neural networks, and testing the relation between the correlation of the activities of the coupled neural groups and the strength and nature of these couplings. Neural networks provide a method of setting up a model neural system where all connections are known in advance. Then by correlating the signals from the model neural dynamics one can investigate to what degree these correlations reflect the connectivity.

Mutual connections between the two networks can be excitatory, inhibitory or nonexistent, and a second question we are investigating here is to what degree one can deduce the nature and possibly the strength of the mutual connections on the basis of the cross-correlation analysis. As we consider throughout the present work the simplest possible network layouts, our conclusions concern the effective connectivity of the networks (Aertsen et al. 1989).

The effect of correlated neural activities caused by synaptic interconnections is difficult to isolate from the synchronization imposed by a common input or, more generally, by correlated inputs to the two systems (Palm et al. 1988). The linear partialization method (van Dijk 1995) can subtract the influence of the correlated source from the cross-correlation functions as long as we can assume that the response to the external source is linear. This last condition can be verified for loosely connected networks. In the case of highly interconnected neural systems, for example when oscillatory behavior is present, the response is far from linear. In such cases,

Correspondence to: B. W. van Dijk, Laboratory for Medical Physics, University of Amsterdam, Meibergdreef 9, 1105 AZ Amsterdam, The Netherlands (e-mail: b.vandijk@amc.uva.nl)

therefore, any conclusions for the functional connectivity between two neural systems that are based solely on the presence of correlated activity are questionable. Here we explore this problem also, by simulating the activities of two neural networks in the presence of a common input. We show that if the common input is of a rate smaller than the characteristic oscillation frequency of the systems then linear partialization can still reveal the correlations due to the synaptic interactions.

Our model neural networks are randomly connected with all neurons projecting and receiving synaptic connections with the same probability. The behavior of the network and in particular its response to external inputs will depend on the connectivity, the balance between excitatory and inhibitory connections, and the dynamics of these connections. In the situation where the networks are densely connected, it is natural to expect oscillatory behavior. In this 'strong coupling limit', if a system is constantly excited by a stochastic external input, it responds with spontaneous bursts. These bursts will appear in some approximately periodical fashion. In such an approach the oscillations appear naturally as a result of the collective neural dynamics. Each individual neuron does nothing more than integration of synaptic signals and producing corresponding action potentials. There are no bursting properties involved in the dynamics of a single neuron. Yet when such neurons are interconnected to form networks, these networks can have oscillatory behavior with different frequencies (burst-to-burst intervals), amplitudes and burst lengths. Oscillatory networks are of special interest and some authors suggest that they may provide a tool for understanding the mechanism of feature-linking in biological sensory systems (Eckhorn et al. 1988; Chawanya et al. 1993; for a recent review see Eckhorn 1994).

Consider now two neural networks, each densely connected internally. When the two neural networks are disconnected from each other, even if their mean bursting rates are the same, they will burst noncoherently and therefore their cross-correlation function will be zero. It is easy to conclude that the two oscillating systems have zero correlations because of the accumulating stochastic phase distances of the sequentially ordered bursts. Excitatory synaptic interactions between the two networks can cause partial or complete synchronization of the activities, depending on the strength of these connections. Ultimately, the two oscillating systems merge into one. To see this, one can simply compare the autocorrelation functions of both systems with their cross-correlation function. This analysis forms our first set of results.

When the two networks interact with inhibitory synapses also, the correlation picture is different. Inhibition causes synchronization between the two oscillating systems but in an anti-phase fashion. It leads also to a decrease in the oscillation period of both systems. We trace how this evolves when, parallel to the inhibition, an excitatory interaction is gradually taking over. We show that the transition from anti-phase to in-phase coherency is accompanied by an increase in the oscillation frequency by a factor of approximately 2.

Correlation between the neural activities can also be a consequence of a common input. Suppose that during a short epoch synchronous impulses are affecting both networks simultaneously with a stochastic input. Each impulse will cause in most cases (unless one or both of the systems is deeply inhibited after a previous burst) an induced burst from both networks. If the systems are isolated, the next bursts will come with phases increasingly fluctuating around the mean burst-to-burst period, and in time the systems will regain uncorrelated bursting. If the external pulse 'synchronization' is with a rate much lower than the mean frequency of the oscillating networks, we expect the correlations thus induced between the systems to be, at a first approximation, linearly superimposed with those caused by the synaptic interactions. In such a case the influence of the common input can be subtracted from the correlation functions with linear partialization techniques.

The last objective of this work was to determine to what extent and under what conditions the partialized cross-correlation function between the firing activities of two oscillating networks still carries information about the mutual synaptic connections. When we affected each of the networks with periodic external pulses, we observed that the networks responded with bursts coming sequentially with the same frequency as the input, as long as this frequency is smaller than that of the spontaneous (in the presence of noisy input) oscillations. In this condition we found that the partialized cross-correlation function carries information about the synaptic connections. Above this threshold the networks respond with bursts coming at fractional frequencies. In this regime, the partialized cross-correlation function no longer reflects the synaptic interactions between the systems.

2 Methods

2.1 Correlation analysis

A measure of the linear correlation between two signals $s_i(\tau)$ and $s_j(\tau)$ is their cross-correlation function (CCF), defined as

$$D_{ij}(t) = \frac{d_{ij}(t)}{\sqrt{d_{ii}(0)\, d_{jj}(0)}} \tag{1}$$

where

$$d_{ij}(t) = \lim_{T\to\infty} \frac{1}{2T} \int_{-T}^{+T} (s_i(\tau) - \langle s_i\rangle) * (s_j(t+\tau) - \langle s_j\rangle)\, d\tau = d_{ji}(-t) \tag{2}$$

and $\langle s_i\rangle$ is the mean value of the ith signal.

In the case of $i = j$ we obtain the autocorrelation function (ACF) of a given signal.

The normalization is chosen so that for uncorrelated (statistically independent) signals we have $D_{ij}(t) = 0$ for all correlation times, and for completely correlated signals we have $D_{ij}(0) = 1$.

In this work we applied the discrete form of (1) for our simulated signal sequences, correcting the normalization for the finite number of samples.

Suppose now that both channels are influenced by a third signal. To subtract this influence from the CCF to a linear order one can perform a linear partialization. The partialized CCF between signals s_i and s_j, accounting for the influence of signal s_k, is given in the Fourier-trans-

formed form as (Bendat and Piersol 1968)

$$D_{ij|k}(\varpi) = D_{ij}(\varpi) - \frac{D_{ik}(\varpi) * D_{kj}(\varpi)}{D_{kk}(\varpi)} \tag{3}$$

Here all CCFs are Fourier transformed.

It is clear that (3) can be obtained by subtracting from ith and jth signals their linear predictions from the kth signal.

We used this partialization technique with all Fourier components above a 60-Hz cutoff. This was done to avoid division by small numbers errors that can penetrate in (3) through the division by the ACF spectrum.

The interpretation of the partialized CCF (3) is that it holds the remaining information about the functional correlation between the two systems after the common input influence has been removed in linear approximation. This formula can be straightforwardly extended to the case of many correlated input patterns affecting one or both systems. To keep the analysis simple, we consider here only the case where there is one external input exciting both networks simultaneously.

2.2 Signal generation: network layout

Half the neurons were taken to be excitatory and half the units were taken as inhibitory. The only difference between the neurons is that the excitatory neurons project only via excitatory synapses while the inhibitory neurons can only inhibit by their synaptic projections. The internal connectivity of each of the networks was chosen to be diffuse. The average number of connections to neurons of the same network per neuron was 70. Mutually the two networks can be connected only with excitatory synapses or with excitatory and inhibitory synapses. Each neuron had on average 20 projections to neurons of the other network. The synapses of inhibitory type are taken to have the same synaptic strength [see (7)], irrespective of whether the connection is between two neurons from the same network or different neural networks. In all simulations where the two networks excite each other, the synaptic strength of an excitatory projection to the other network measures the connectivity strength between the two systems. This quantity was set as a fraction of the synaptic strength set for the internal excitatory synapses. This fraction (a parameter taking values between 0 and 1) is then taken as a measure of the relative connectivity between the networks (related to the internal connectivity).

External input to the two networks is transferred through a separate set of excitatory synapses at random neurons. In our layout about 80% of the neurons received external input. Two different types of inputs were applied. In all simulations, a stochastic, noisy signal was fed to both networks. Its level (the probability that an input synapse receives a signal in any time step) was taken such that the systems had clear oscillatory behavior. The noisy input is completely uncorrelated and serves only to provoke the oscillatory regimes for the networks.

In some of the simulations, specified in the next section, we superimposed on this stochastic input pulses presented simultaneously to all input synapses. These synchronized inputs were in all cases of length 6 ms and were presented at random time intervals with mean rates of about 2 Hz.

2.3 Neural dynamics

The dynamics of the individual neurons is chosen to reflect the synaptic integration and action potential generation of real neurons. The detailed model is described below and the parameter settings are given in the Appendix.

Each individual neuron is represented by a set of three compartments as illustrated in Fig. 1a. One of the compartments contains all synaptic channels, both excitatory and inhibitory, and represents the dendrites of the neuron. Synaptic channels are modeled by resistors that change their conductance in response to a presynaptic action potential. The second compartment has a buffering role, has only passive channels and represents the apical dendrite of the neuron. The third compartment contains nonlinear voltage-driven membrane channels. This last compartment, representing the soma and axon, is involved in the production of action potentials.

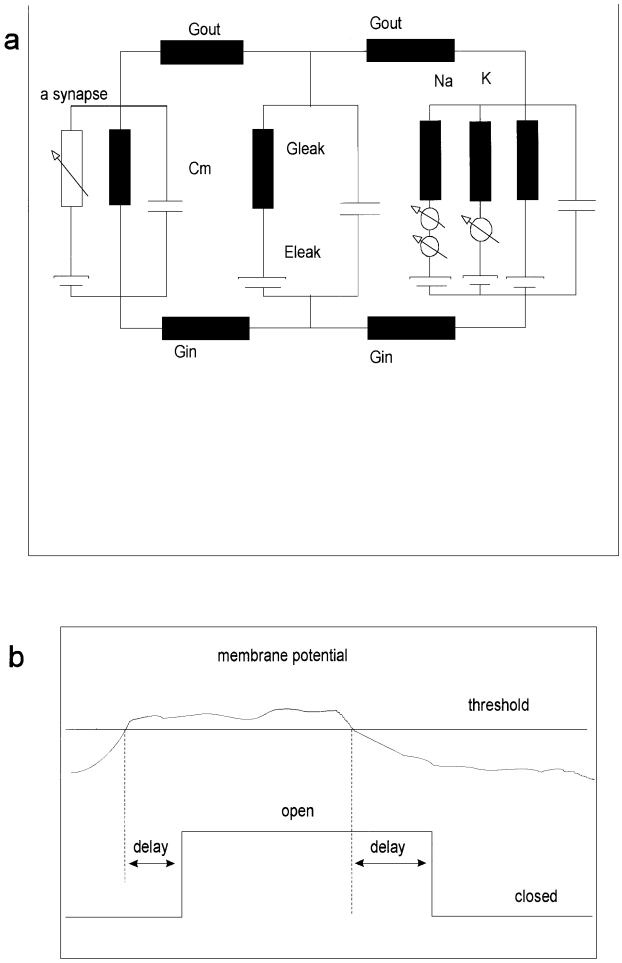

Fig. 1. **a** The model neuron consists of three compartments, interconnected through resistors. The leftmost compartment receives all the synaptic inputs (excitatory and inhibitory) through variable resistors. The central compartment has only passive electrical channels and its role is to decrease the influence of the sharp action potentials on the synaptic channels. Action potentials are generated only in the rightmost compartment, where the voltage-driven binary channels are located. These channels are controlled by sets of binary gates with threshold-type dynamics as explained in the text and in **b**. **b** The time curve illustrates the dynamics of a binary opening gate. When the membrane potential (*curved line*) rises above the threshold value (*horizontal line*) the gate opens after a delay of $\tau_{\text{delay}}^{\text{open}}$. If the potential drops below the threshold, the gate closes after $\tau_{\text{delay}}^{\text{close}}$. In general the threshold for opening the gate can be different from that for closing the gate; in our model cell, however, we have chosen identical values for these thresholds

The transmembrane potential V^i in each compartment obeys the equation

$$C_i dV^i/dt = \sum_{\alpha} G_\alpha(V^i, t)\cdot(E_\alpha - V^i) + \sum_{i<>j} \frac{G_{ij}^{\text{ex}} G_{ij}^{\text{in}}}{G_{ij}^{\text{ex}} + G_{ij}^{\text{in}}}(V^j - V^i) \tag{4}$$

The first sum on the right-hand side of (4) represents the current flowing through the different ion channels (labeled by α) in the ith compartment. The second sum accounts for the current exchange with the neighboring compartment(s). C_i is the membrane capacitance in the ith compartment, G_α is the conductance of the αth channel (in general it can be both voltage and time dependent), and E_α is the Nernst potential characterizing the corresponding channel.

The dynamics of the nonlinear channel conductances can be described by the set of Hudgkin-Huxley equations. Instead we took

a computationally economical approach. For each nonlinear channel we introduced a set (one in the case of the K^+ channel and two in the case of the Na^+ channel) of binary gates represented by a variable $s_\alpha^a(t) \in \{0, 1\}$ which tells whether the gate is open (value 1) or closed (value 0). The channel conductance is then postulated in this approach as an expression of the form

$$G_\alpha(t) = G_\alpha^{\max} \prod_{a,\, b} s_\alpha^a(t) \cdot (1 - s_\alpha^b(t)) \tag{5}$$

where the maximal conductance of the channel, $G_\alpha^{\max}$, is a constant. Clearly, if a channel does not have gates at all, then its conductance is a constant and it will correspond to one of the passive channels on the cellular membrane.

Gates with index a in (5) are opening gates in the sense that they must be open in order for the whole channel to be open. Index b labels closing gates. So a channel is open if all opening gates are open and all closing gates are closed. The dynamics of any channel is determined by the dynamics of the associated gates. The last are given by the following simple rule (channel and gate indexes are omitted below). To each type of gate we attach four constants: $V_{\text{threshold}}^{\text{open}}$, $V_{\text{threshold}}^{\text{close}}$, $t_{\text{delay}}^{\text{open}}$, $t_{\text{delay}}^{\text{close}}$. The dynamics of the binary gate is then described as follows: If a gate is closed initially, the condition to open it is that the transmembrane potential stays above $V_{\text{threshold}}^{\text{open}}$ longer than $t_{\text{delay}}^{\text{open}}$. The condition for closing an open gate is that the potential must stay below $V_{\text{threshold}}^{\text{close}}$ for a time interval longer than $t_{\text{delay}}^{\text{close}}$. The gate dynamics is illustrated in Fig. 1b.

In fact the binary description of the voltage-driven channels is very close to the description given by the Hodgkin-Huxley equations. In these, the channel is presented as a statistical ensemble of binary gates driven by a number of 'particles' that open or close the gates. To make the parallel, in our approach all gates open or close simultaneously but with a delay which replaces the statistical dynamics.

The operation of a synapse can be described by a single second-order equation. The only dynamic variable, $g(t)$, can be considered to represent the concentration of the neurotransmitter near the postsynaptic membrane. The dynamics of the synaptic channel conductance is then described by the equations:

$$\frac{d^2}{dt^2} g(t) + \frac{2}{\tau} \frac{d}{dt} g(t) + \frac{1}{\tau^2} g(t) = \sum_i \delta(t - t_i) \tag{6}$$

$$G_{\text{syn}}(t) = G_{\text{syn}}^{\max} g(t) \tag{7}$$

In (7) $G_{\text{syn}}(t)$ is the synaptic channel conductance that must be entered in (4). $G_{\text{syn}}^{\max}$ is an overall coefficient representing the 'strength' or the efficiency of the particular synapse.

Different types of synapses (e.g., excitatory or inhibitory) are characterized by different channel properties ($G_{\text{syn}}^{\max}$, $E_\alpha^{\text{synapse}}$ and τ), but at rest they are treated uniformly. The set of parameter values used for the actual simulations is listed in the Appendix.

To summarize, the dynamics of the neuron is based on the conductance properties of the various channels in the compartments. Four basic channel types have been used in the model:

$G_{\text{P}} = G_{\text{P}}^{\max}$ for all passive channels

$G_{\text{K}}(t) = G_{\text{K}}^{\max} s_{\text{K}}^a(t)$;

$G_{\text{Na}}(t) = G_{\text{Na}}^{\max} s_{\text{Na}}^a(t)\,(1 - s_{\text{Na}}^b(t))$ for the active channels

$G_{\text{syn}}(t) = G_{\text{syn}}^{\max} g(t)$ for the synaptic channels

3 Results

In the first set of simulations we emulated the system dynamics for ten different levels of excitation between the two networks and no mutual inhibition. The level of mutual excitation represents the relative strength of the (excitatory) synapses transmitting signals from one network to the other. In Fig. 2 we present the CCF between the activities of the two networks for the different excitation levels and the ACF for each of the systems. Our results clearly indicate that the two systems exhibit oscillatory behavior. When the mutual connectivity is zero or beneath a certain threshold, the systems oscillate independently, and because of the independently distributed fluctuations of the burst-to-burst intervals, the CCF [see (2)] is zero. When the connectivity is higher than this threshold the two systems synchronize their bursting patterns. For networks that are strongly connected to each other this results in a CCF that is almost identical with both the ACFs.

It is also clear that the two networks, when uncoupled, can have not only different phases but also different burst-to-burst average periods. This is reflected in the difference between the ACFs of the two networks (the bottom line in Fig. 2) and is due to the fact that the two networks are not completely identical. Strong mutual excitation causes both oscillators to 'negotiate' a common frequency and common duration of the single bursts and, finally, synchronizes their phases. In the intermediate stages of this transition, when the coupling parameter is in the range 0.5–0.6, the networks still retain their individual patterns of activity as indicated by the asymmetric shape of the CCFs in Fig. 2.

In the second set of simulations, presented in Fig. 3, we set a constant level of mutual inhibition between the two networks. The probability of an inhibitory neuron from each of the networks sending a projection to a given neuron from the other network is taken to be 0.2. The excitatory neurons were assumed to send projections to the other system with the same probability. All the inhibitory synapses between the two systems were set with fixed synaptic efficiencies while the excitatory synapses were taken with ten increasing efficiency values, the same as in the previous set of simulations. From the CCFs and ACFs presented in Fig. 3 we see that when inhibition dominates, the two oscillating networks burst in anti-phase. In other words, the bursting of one of the systems takes place when the other system is inhibited, and vice versa. When the excitation gradually takes over, the systems start oscillating in phase. There is no actual shift in the phases, though. The transition from anti-phase to in-phase coherent oscillation takes place by doubling the frequency, or in other words additional bursts emerge in between every two successive bursts present in the case with mutual inhibition only. There is no level of excitation that can compensate for the mutual inhibition, so that the two networks fire independently.

In the next two sets of simulations we introduced a common input to both networks. The connections were the same as those of Figs. 2 and 3. The input signal consisted of noise with superimposed pulses given simultaneously to both systems in a random sequence. The mean rate of the external common pulses was taken to be 2 Hz. This value is smaller than the oscillation rate of the networks.

The simultaneous input causes correlations between the activities of the two networks. The CCFs are presented in the left column in Figs. 4 and 5 for the cases without and with mutual inhibition, respectively. Now the question is to what extent we can account for the external

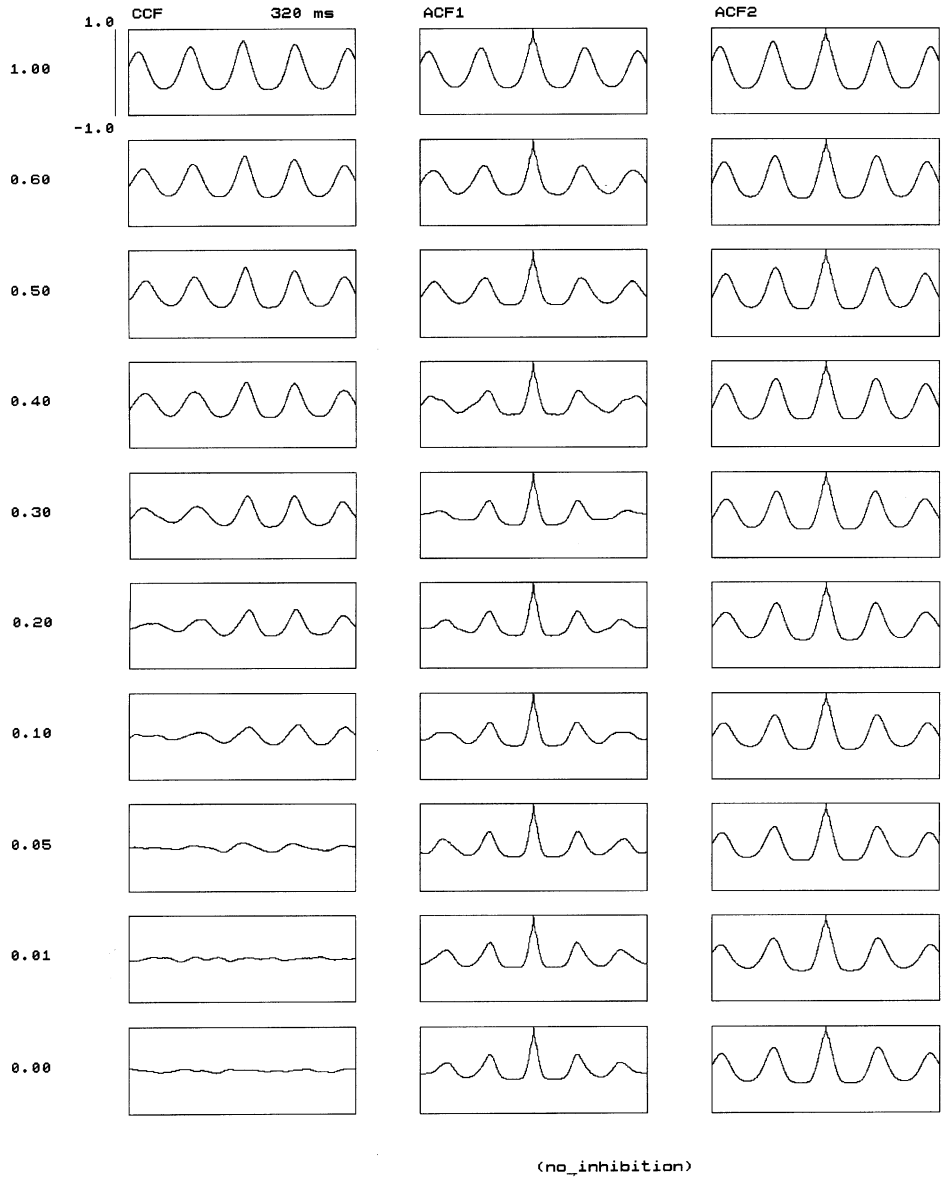

Fig. 2. In this set of simulations the dynamics of two neural networks were simulated. Each network consisted of 50 excitatory and 50 inhibitory neurons and the internal connectivity was 70% (each neuron projects synapses to 70 other neurons of the same network). The networks were mutually connected reciprocally with only excitatory synaptic connections, of efficiencies chosen differently for the different simulation sessions. The mutual connectivity for all simulations was set to 20%. The *first column* represents the cross-correlation functions; the *second* and the *third columns* represent the autocorrelation functions of the first and the second system correspondingly. Each *row* of correlation functions is obtained from a separate simulation session. Different sessions are characterized by different values of the efficiencies of the synapses connecting the two systems. The efficiency of each synapse connecting the two networks, or its maximal conductance [see (2.7)], is set as a fraction of the value $G_{\text{syn}}^{\max}$ given in the Appendix. These fractions are shown in front of each horizontal row of correlation functions. During the simulations, a stochastic (noncorrelated) excitatory noise was applied to both systems to provoke spontaneous oscillations. It is clear that the (excitatory) connectivity between the systems causes synchronization between the oscillators. There is little effect of this synchronization on the oscillatory pattern (ACF) of each of the individual networks. All functions here and in the subsequent figures are normalized according to (1) and their values are in the interval $(-1.0 \ldots 1.0)$

synchronization and restore the connectivity-dependent correlations from Figs. 2 and 3. To answer this question, we performed a linear partialization of the CCF of the two systems with respect to the common input according to (3). The partialized CCFs are presented in the middle column in Figs. 4 and 5. Comparing these partialized CCFs with the corresponding CCFs from Figs. 2 and 3, we see that the influence of the common input on the CCF can be taken into account and the partialized CCF between the activities of the two systems carries information about the mutual connectivity.

We also observe that in all cases in this simulation set, the linear parts of the correlations caused only by the common input [the second term in the right-hand side in (3) and presented as the right-hand column of CCFs in Figs. 4 and 5] are almost identical. This verifies the assumption in Sect. 1 that we can account for the external input with linear techniques.

Our last set of simulations was aimed at determining the limits of the partialization method. In this set of simulations we considered two networks completely disconnected from each other. The only external input is a periodic sequence of pulses, each of length as above (i.e., 6 ms), but arriving at different frequencies. There is no noisy input fed to the systems (and therefore there were no spontaneous oscillations present). The left-hand column of Fig. 6 shows the ACFs of one of the systems for different input frequencies. We see that up to input frequencies of 25 Hz, the output of the neural systems follows the input rate. At frequencies above this value the system cannot follow the input rate and responds with some fractional bursting frequency.

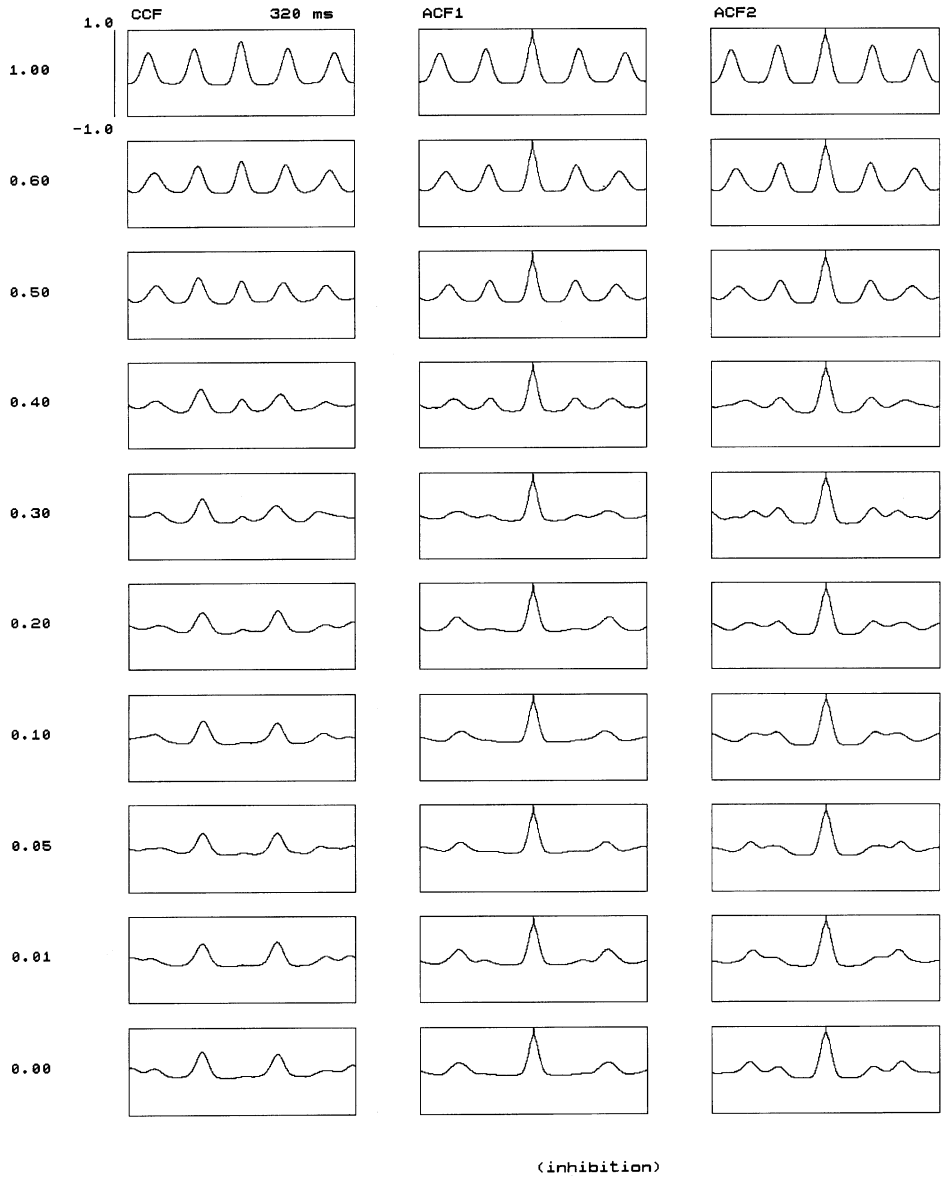

Fig. 3. The same layout as in Fig. 2 was simulated, but here the two systems were connected also with inhibitory synapses, with fixed efficiencies for all sessions. The excitatory connections between the networks were set for the different sessions with different synaptic efficiencies equal to the corresponding ones from the simulations in Fig. 2. These results show that when the two networks inhibit each other, the corresponding oscillators anti-synchronize (oscillate in anti-phase). With the increase in the excitatory component in the mutual interaction, the oscillations double their frequencies and synchronize their phases

For the same set of simulations the middle column of Fig. 6 shows the CCF between the two completely isolated systems. The only correlations between the activities are caused by the periodic input. Partialized CCFs are shown in the right-hand column of Fig. 6. We see that for frequencies below 25 Hz, the partialization gives the correct result – zero residual correlations, indicating zero connectivity. At input rates above this frequency, the linear partialization is no longer applicable.

4 Discussion

In this paper we show that synaptic connections between two densely interconnected neural networks determine the cross-correlation function between their firing activities. Inversely, if the networks exhibit oscillating behavior, their connections can be deduced from the shape of the CCF. If their CCF returns to zero, then they are at most weakly connected. If the CCF is that of two synchronous oscillators, then the networks are exciting each other. A third possibility, where the CCF shows two oscillators bursting with the same intervals but in 'anti-phase', reveals mutual inhibition.

We see from the first column of CCFs in Fig. 2 that weakly correlated activities result first in a nonsymmetric CCF. This show that although the two systems start to synchronize their bursting patterns, they still behave as two separate systems. A fully symmetric CCF is an indication that the effective connectivity between the two networks is at a level such that the two systems are dynamically equivalent to a single oscillator.

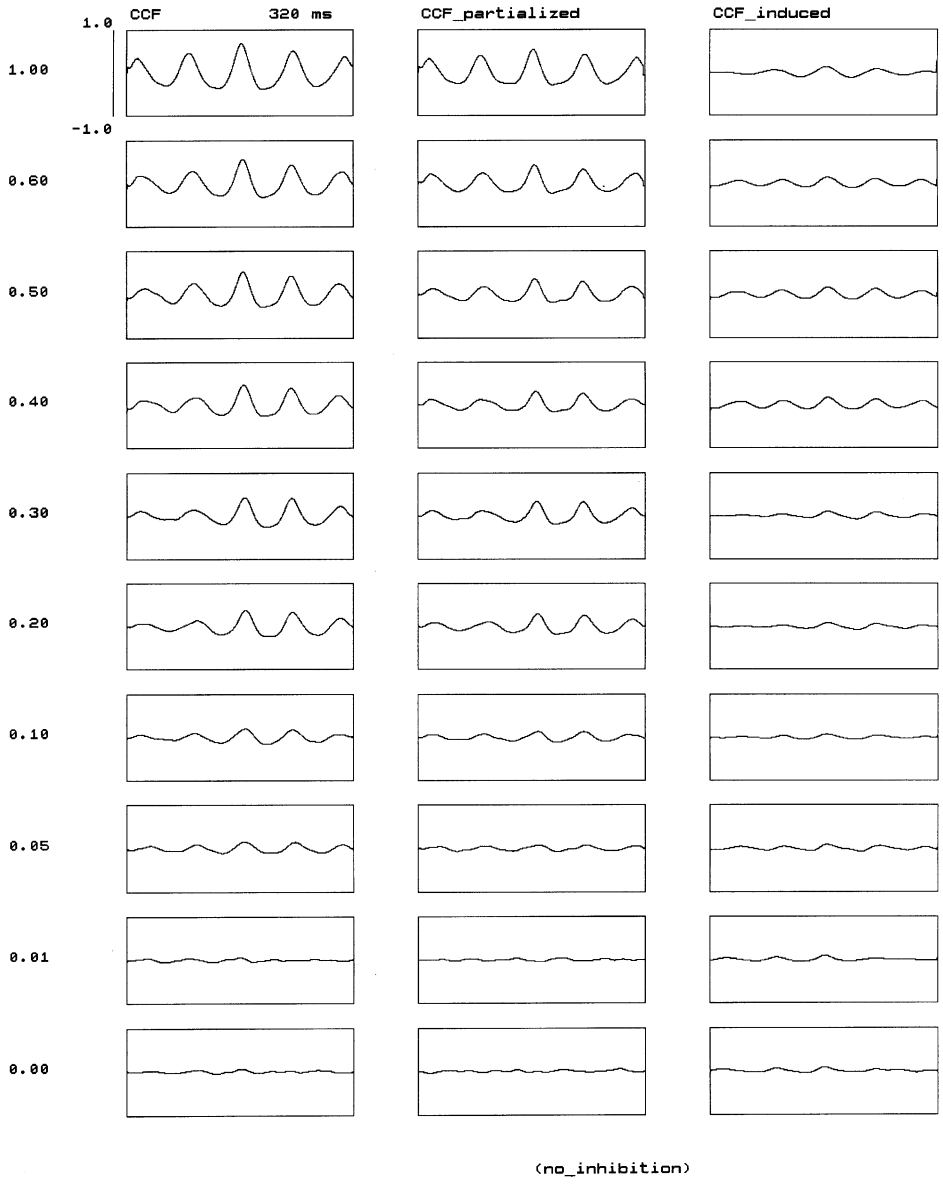

Fig. 4. Partialized cross-correlation functions (*left column*) were simulated for two neural networks connected reciprocally with excitatory synapses at different efficiencies. An excitatory external common input is applied simultaneously to the systems. The input is in all cases a random (nonperiodic) sequence of excitatory pulses of length 6 ms and mean rate 2 Hz. During all the simulations stochastic (noncorrelated) excitatory noise was in addition applied to both systems to provoke spontaneous oscillations. The *left column* represents the CCF. The *middle column* represents the partialized correlation functions between the activities of the two networks. The *right column* shows the difference between the nonpartialized and the partialized CCFs and reflects the influence of the common input on the correlated activities. Since the common input is the same for all simulations, its influence should in a linear regime also be identical. Each *row* of correlation functions is obtained from a separate simulation session. Different sessions are characterized by different values of the efficiencies of the synapses connecting the two systems. The efficiency of each synapse connecting the two networks, or its maximal conductance [see (7)], is set as a fraction of the value G_{syn}^{max} given in the Appendix. These fractions are shown in front of each horizontal row of correlation functions

Similar conclusions can be drawn from the first row of CCFs in Fig. 3. A symmetric CCF, but with a dip around the zero time lag, indicates systems coupled with strong inhibitory connections. The two oscillating systems are phase-locked to each other in an anti-phase manner. The appearance of a central peak in the CCF shows an excitatory 'component' in the effective connection between the networks. When excitation reaches certain level, the two systems form, as in the previous case, a single oscillating system.

These conclusions are valid even when an external common input causes part of the correlated activity. If this input arrives at rates lower than the bursting frequencies of the networks, a linear partialization of the CCF 'cleans' the correlation picture and provides information about the mutual synaptic interaction. Because the above method is based on the assumption of a linear superposition of the correlation functions, it can be correctly applied only when the input causes 'linear perturbations' of the activities of the systems. This can be the case, for example, for an internally loosely connected network, responding linearly to an external signal.

In our case, the two oscillating networks behave nonlinearly. If the external signal is beneath a certain threshold, the networks will show little response. Above this threshold, each of the networks will respond with repetitive bursts for as long as the external signal is on. The amplitude and the frequency of these bursts are almost independent of the strength of the external signal. Nevertheless, if the spontaneous activity is low and the external input is of a low rate, the partialization method

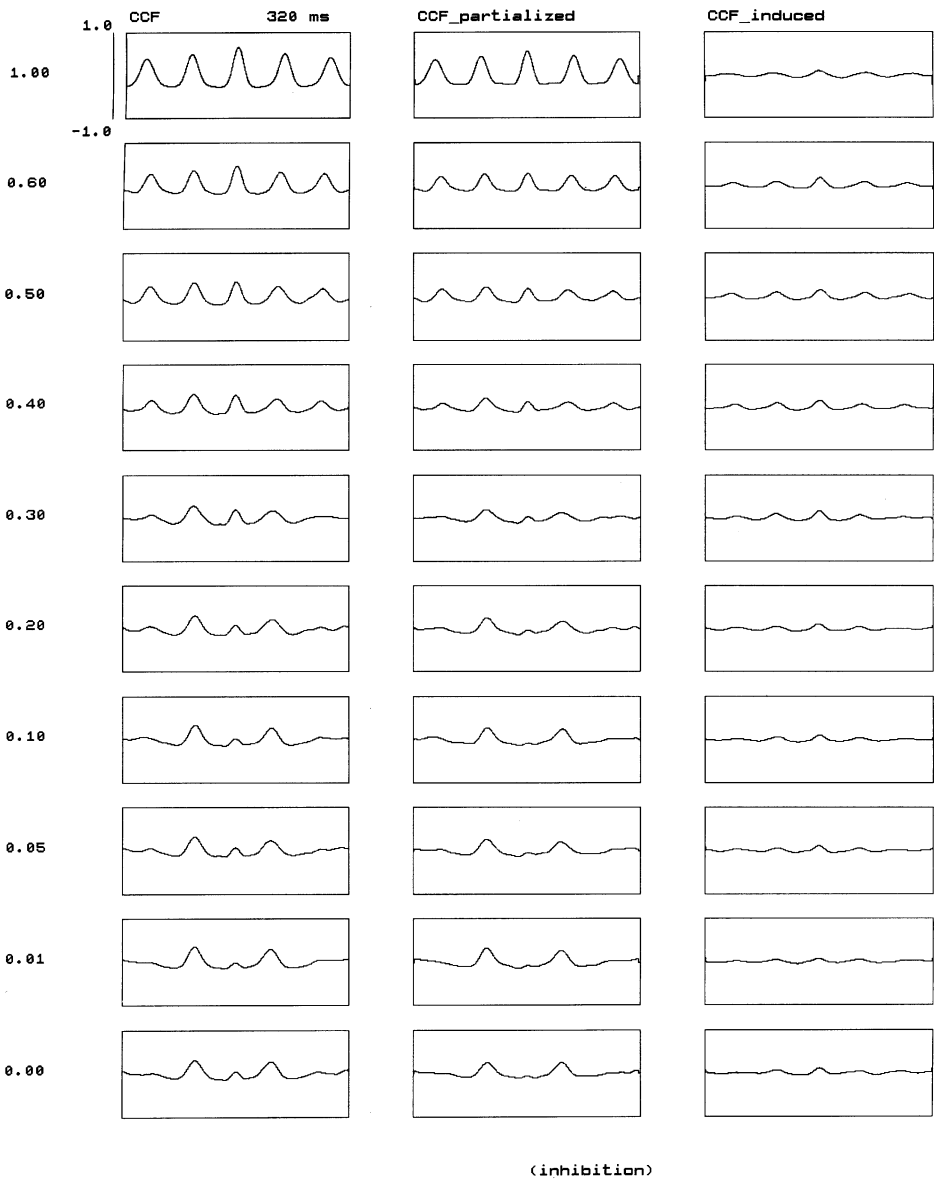

Fig. 5. The same simulations were performed as in Fig. 4, but here the two systems were connected also with inhibitory synapses, with efficiencies fixed for all sessions. The excitatory connections between the networks were set for the different sessions with different synaptic efficiencies equal to the corresponding simulations in Fig. 4. In this set of simulations the effect of partialization is particularly clear in cases with predominant inhibition. The CCFs in the *middle column* have a central hatch which represents the synchronization effect of the common input. It is completely removed in the partialized CCFs (*middle column*). The influence of the common input on the CCFs (*right column*) is found to be of the same order for all levels of mutual connectivity, which shows that this influence can be considered, in a first approximation, as linear

can still be applied successfully. The reason is that in the above circumstances the probability of spontaneous (eventually repetitive) bursting and simultaneously an induced response to the input is very small. Therefore, the two causes contributing to the shape of the CCF act independently and their effects are superimposed in a linear way. When the spontaneous activations and/or the rate of the external source increase, the CCF between the two systems ceases to be a linear superposition of an induced plus an internal part and the partilization method will fail.

Another limitation of the linear partialization method is that it is applicable only to experimental situations where the possible source of external synchronization is known – as, for example, in experiments with visual or other sensory stimulation.

Our conclusions hold for a wide range of parameter settings in the artificial neural network. One crucial condition is that each of the networks is sufficiently intrinsically connected both with excitatory and with inhibitory synapses. This will ensure a unimodal oscillatory response to external perturbations. The connectivity between the networks is taken to be sparse in comparison with the internal connectivity. The parameters chosen for the dynamics of the individual neuron ensure a sigmoidal effective response of the neuron to external excitations. The explicit modeling of the synaptic channels as well as of the nonlinear voltage-driven channels (only the minimal set is considered in this paper) in a realistic, but computationally economic way, provides the opportunity to investigate the role of the individual membrane channels in large-scale network behavior.

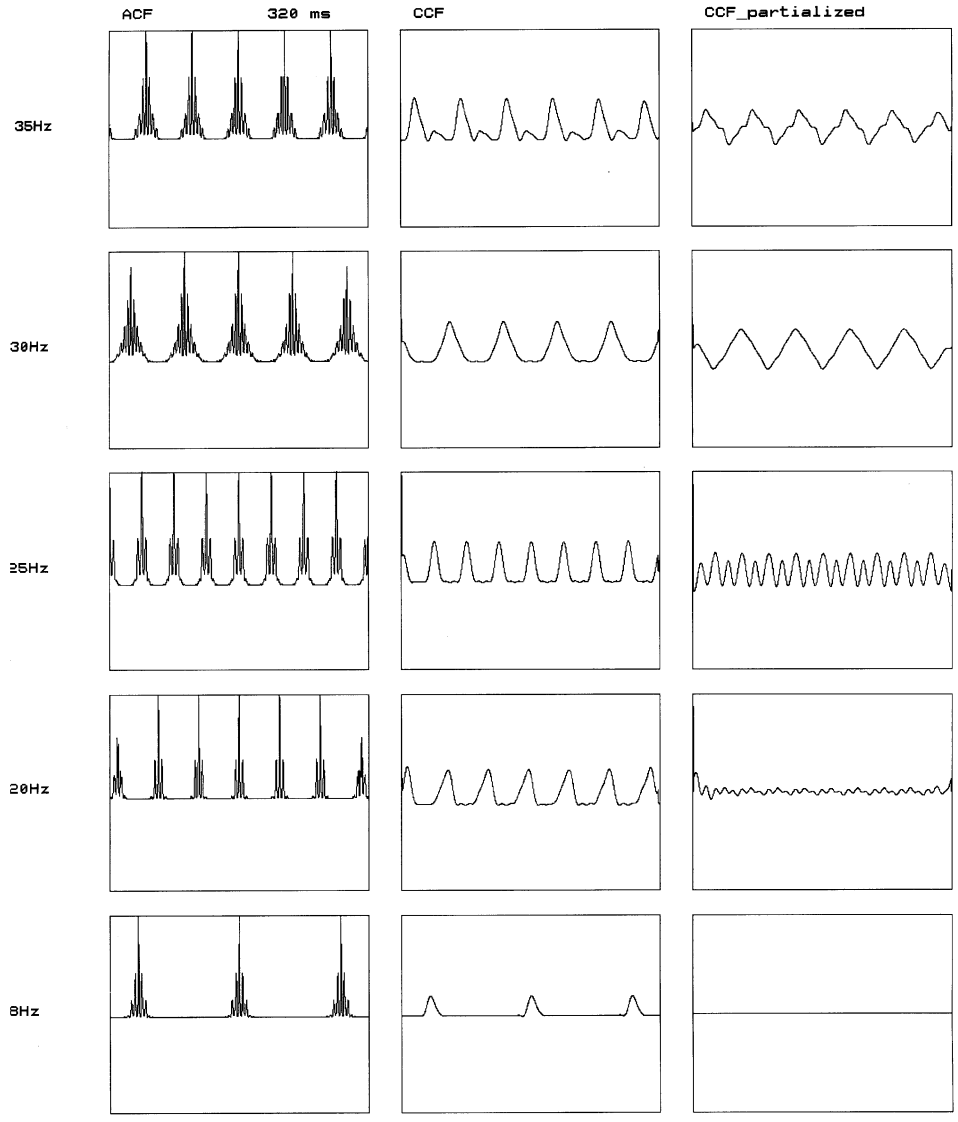

Fig. 6. Simulations testing the responses of the model network were performed with periodic external input with different frequencies. The input consists of a periodic sequence of pulses (length 6 ms). The frequency of the pulses was taken to be different for the different sessions; values are denoted in front of each horizontal row on the figure. No noisy external signal was applied during these simulations. The *left column* presents the autocorrelation functions of the activity of a model neural network. The figure shows that up to frequencies of 25 Hz of the input, the network responds with periodic bursts of the same frequency. For higher input frequencies, the network respond with a fraction of the input frequency. The *middle column* represents the cross-correlation functions between the activities of the networks. The *right column* represents partialized correlation functions. As all the correlations are caused only by the common input, partialized CCF should be zero for all correlation times. We see that this is the case for input frequencies up to 25 Hz. Above this input rate, the linear partialization method fails to account for the common input

Appendix

Here we give the parameters used to describe the model neuron [see Fig. 1 and (4), (5) and (7)].

All differential equations were integrated with a Euler-forward method. The elementary time step was postulated to be 0.1 ms.

In all compartments the *capacitance* is taken to be:

$$C_i = 1[nF]$$

Channel parameters:

Channel	G_0 (mS)	E (mV)	τ (ms)	Gates
Passive	0.3	− 54.4	–	–
Excitatory	12.0	− 10.0	4	–
Inhibitory	3.0	− 55.0	8	–
Na^+ active	1.2	+ 50	–	*a*, *b* type
K^+ active	1.6	− 77	–	*a* type

For all channels, G_0 is the nominal conductance. Synaptic channel conductance is modulated by the function $g(t)$ as presented in (7). Nonlinear, voltage-driven channels are controlled by their *gates parameters*. These are:

Gate	$V^{\text{open}}_{\text{threshold}}$	$V^{\text{close}}_{\text{threshold}}$	$t^{\text{open}}_{\text{delay}}$	$t^{\text{close}}_{\text{delay}}$ (ms)
Na^+ *a* gate	− 45.0	− 45.0	0.1	0.1
Na^+ *b* gate	− 35.0	− 35.0	0.4	0.4
K^+ *a* gate	− 30.0	− 30.0	0.5	0.5

The electrical links between the compartments are specified by their conductances, and the quantity that is entered in (4) is $\Gamma = G_{\text{in}}G_{\text{out}}/(G_{\text{in}} + G_{\text{out}})$.

Thus, for the link between (cf. Fig. 1) the synaptic and the second (buffering) compartment we have chosen $\Gamma = 1.5$ and for the link between the buffering and the active compartment we have chosen $\Gamma = 0.5$.

References

Aertsen AM, Gerstein GL (1985) Evaluation of neuronal connectivity: sensitivity of cross-correlation. Brain Res 340:341–354

Aertsen AM, Gerstein GL, Habib MK, Palm G (1989) Dynamics of neuronal firing correlation: modulation of 'effective connectivity'. J Neuro-physiol 61:900–917

Bendat SJ, Piersol AJ (1968) Measurement and analysis of random data. Wiley, New York

Chawanya T, Aoyagi T, Nishikawa I, Okuda K, Kuramoto Y (1993) A model for feature linking via collective oscillations in the primary visual cortex. Biol Cybern 68:483–490

Eckhorn R (1994) Oscillatory and non-oscillatory synchronizations in the visual cortex and their possible roles in associations of visual features. Prog Brain Res 102:405–426

Eckhorn R, Bauer R, Jordan W, Brosch M, Kruse W, Munk MH-J, Reitboek HG (1988) Coherent oscillations: a mechanism of feature linking in the visual cortex? Multiple electrode and correlation analyses in the cat. Biol Cybern 60:121–130

Eckhorn R, Schanze T, Brosch M, Salem W, Bauer R (1992) Stimulus-specific synchronization in cat visual cortex: multiple microelectrode and correlation studies from several cortical areas. Bullock TH, Basar E (eds) Induced rhythms in the brain. (Springer series in brain dynamics) Springer, Berlin Heidelberg New york

Gray CM, Engel AK, König P, Singer W (1992) Synchronization of oscillatory neural responses in cat striate cortex: temporal properties. Vis Neurosci 8:337–347

Nelson JI, Salin PA, Munk MH-J, Arzi M, Bullier J (1992) Spatial and temporal coherence in cortico-cortical connections: a cross-correlation study in areas 17 and 18 in the cat. Vis Neurosci 9:21–37

Palm G, Aertsen AM, Gerstein GL (1988) On the significance of correlations among neuronal spike trains. Biol Cybern 59:1–11

Singer W (1993) Synchronization of cortical activity and its putative role in information processing and learning. Annu Rev Physiol 55:349–374

Spekreijse H, Dijk BW van, Vijn PCM, Kalitzin SN (1994) Non-linear dynamics of columns of cat visual cortex revealed by simulation and experiment. In: Bochk JR, Gosde JA (eds) Higher-order processing in the visual system (CIBA foundation symposium) John Wiley & Sons, Chichester New York Brisbane Toronto

van Dijk BW (1995) Synchrony and fast plasticity in the visual cortex. In: Kappen B, Gielen S (eds) Neural networks of artificial intelligence and industrial applications. Springer, Berlin Heidelberg New York